Antimicrobial, Polarizing Light, and Paired Helical Filament Properties of Fragmented Tau Peptides of Selected Putative Gingipains

Shalini Kanagasingam[a], Christopher von Ruhland[b], Richard Welbury[a] and Sim K. Singhrao[a,*]

[a]*Brain and Behavior Centre, Faculty of Clinical and Biomedical Sciences, School of Dentistry, University of Central Lancashire, Preston, UK*
[b]*Electron and Light Microscopy Facility, College of Biomedical and Life Sciences, Cardiff University, Cardiff, Wales, UK*

Abstract.
Background: Tau is an established substrate for gingipains secreted by *Porphyromonas gingivalis*. Hyperphosphorylation of tau and neurofibrillary tangle (NFT) formation is a defining lesion of Alzheimer's disease (AD) where NFT distribution is related to Braak stage and disease severity.
Objective: To assess gingipains'-fragmented tau peptides for their antimicrobial properties and for the likelihood of paired helical/straight filament (PHF/SF) formation with implications for the NFT lesion.
Methods: Seven non-phosphorylated (A-G) and three phosphorylated (A-C) tau peptides, were tested for antimicrobial properties against *P. gingivalis*. Polarizing light properties were determined using Congo Red staining. Secondary and tertiary structures of peptides B-F were determined using transmission electron microscopy (TEM) and circular dichroism (CD) was undertaken for the soluble peptides A in phosphorylated and non-phosphorylated states.
Results: Phosphorylated tau peptide A displayed a significant effect against planktonic *P. gingivalis*. The CD results demonstrated that both peptides A, in phosphorylated and non-phosphorylated states, in aqueous solution, adopted mainly β-type structures. Non-phosphorylated peptides B-F and phosphorylated peptides B-C were insoluble and fibrillar under the TEM. The secondary and tertiary structures of the non-phosphorylated peptide B demonstrated fewer helical twists, whereas peptide C displayed significantly more helical twists along the whole fiber(s) length following its phosphorylation.
Conclusion: Phosphorylated peptide A reduced *P. gingivalis* viability. CD spectroscopy demonstrated the phosphorylated and the non-phosphorylated peptide A predominantly formed from β-sheet structures in aqueous solution with potential antimicrobial activity. Phosphorylation of tau peptides physically changed their tertiary structure into PHFs with potential for self-aggregation and binding to the NFT lesion.

Keywords: Antimicrobial, β-sheet, birefringence, gingipains, neurofibrillary tangles, *Porphyromonas gingivalis*, tau

INTRODUCTION

Alzheimer's disease (AD) is a major cause of dementia constituting around 60–80% of all cases.

AD can manifest via several pathways as it is comorbid with Lewy body disease, Parkinson's disease [1], other neurodegenerative diseases [2], and stroke/ischemic stroke as well as type 2 diabetes mellitus [3–5]. Diagnosis of AD is based upon clinical symptoms and upon the presence of two microscopical lesions, namely the amyloid-β (Aβ) plaques

*Correspondence to: Sim K. Singhrao, University of Central Lancashire, Preston, PR1 2HE, UK. E-mail: SKSinghrao@uclan.ac.uk.

and neurofibrillary tangles (NFTs) in postmortem brain tissue sections [6]. The antimicrobial protection hypothesis [7] states that Aβ release and its accumulation in AD brain is the result of an initial microbial infection, which could be from multi-species of cross-Kingdom (viruses, bacteria, fungi) microorganisms, including the oral bacterium *Porphyromonas gingivalis*. Notably, however, evidence shows that Aβ peptide is one of a range of antimicrobial peptides which are produced in response to pathogens. *P. gingivalis* has gained prominence due to its ability to induce inflammation peripherally via the oral inflammatory disease, periodontitis [8]. *P. gingivalis* and/or its virulence factors, mainly gingipains and lipopolysaccharide (LPS) located in the outer layer of the membrane, can enter the brain and give rise to neuroinflammation [9, 10]. The brain has a limited ability to deal with microbial pathogens as it relies mainly on its innate immune inflammatory responses [11, 12]. However, other clearance pathways, which work independent of the innate immune system to clear degraded proteins in the brain, have been noted and are reviewed elsewhere by Singhrao and Olsen [11]. The resulting inflammation is thought to enhance the neuronal loss associated with AD. Regarding the gingipain hypothesis, Cortexyme's Atuzaginstat has been reported to decrease the rate of cognitive decline in AD patients with *P. gingivalis* infection, in phase II/III of the GAIN trial at CTAD 2021 [13]. The GAIN trial highlights the potential benefit of Atuzaginstat in mild to moderate AD cases and suggests that this oral pathogen may be involved in the early stages of AD initiation and to some extent in the disease progression. However, the results of the GAIN trial could have been strengthened with the inclusion of tau cerebrospinal fluid levels for phospho-tau 181 (threonine231) and total tau as a biomarker for AD progression.

The present study was encouraged by Kobayashi et al. [14], who reported that several motifs in tau protein had antimicrobial properties. Two of the motifs ("VQIINK" and "VQIVYK") were also present in the gingipains'-fragmented tau peptides and this led us to investigate the antimicrobial phenomenon attached to these two hexapeptide motifs on *P. gingivalis* planktonic cultures.

In AD, phosphorylated tau features in NFTs along the microtubule binding domains of tau constituting paired helical and straight filaments (PHFs and SF). PHFs show twists along their fibers, with the helical part being approximately 20 nm wide, 80 nm apart with the twist being 10 nm long [15]. Neuropil threads

are also associated with AD, and the spread of the NFTs and neuropil thread pathology is considered in Braak staging as mild, moderate, and severe stages of disease progression [16, 17].

The concept that human tissue specific microbiomes can undergo dysbiosis and affect disparate organ pathology, such as the oral-gut microbiome, has associated periodontal pathogenic bacteria with AD development. This is supported by epidemiological and laboratory-based studies [9, 10, 18–20] and with *P. gingivalis* exotoxin gingipains to tau breakdown [10]. Originally, Poole et al. [9] demonstrated *P. gingivalis* LPS in AD brains, some of which, looked like clusters of outer membrane vesicles. The outer membrane vesicles have been reported to carry gingipains and other lesser virulence factors [11]. A literature review by Zhan et al. [21] found evidence for much more bacterial LPS in the AD brain compared to the control brain. Similarly, Dominy et al. [10] identified the DNA for the elusive and suspect bacterium *P. gingivalis* mostly in AD brains. Authors (S.K. Singhrao) have increasingly identified LPS and gingipains in AD brains [9, 10]. Bacterial factors like LPS are potent immune modulators [22] and in the context of NFT biogenesis, can induce immune signaling cascades that indirectly activate glycogen synthase kinase-3β (GSK-3β). This can lead to phosphorylating tau at serine (ser)396 and threonine (thr)231 amino acid residues as reported elsewhere [23, 24].

Excessively phosphorylated tau becomes insoluble and toxic, this provided the rationale to explore the role of the gingipains'-fragmented tau peptides, for a better understanding of their functional and structural characteristics. This concept agrees with the effects of the $A\beta_{1-40/42}$ peptides, which show similar antimicrobial peptide properties [25, 26] and suggests that it is the presence of pathogenic microbes in the brain, which provoke antimicrobial responses via Aβ release and consequently, give rise to neuroinflammation and damage to neurons. *P. gingivalis* is a Gram-negative, anaerobic intracellular bacterium, which is considered a keystone pathogen in periodontitis [27]. LPS with its plethora of virulence factors is a potent stimulator of the host's innate immune signal transduction pathways in a tissue/cell specific manner [22].

There is also accumulating evidence that structure is key in the antimicrobial interaction exerted by peptides such as human $A\beta_{40}$ and $A\beta_{42}$, which appear to possess amyloid-mediated antimicrobial properties [28, 29]. Based on these observations, and to obtain further mechanistic information on the mode

of action of phosphorylated peptides, circular dichroism (CD) experiments were performed in solution and in the presence of trifluoroethanol (TFE) in order to obtain structural information on the soluble tau peptides A.

Tau in the brain is predominantly found in neurons. Human tau undergoes numerous post-translational modifications including phosphorylation [30–32]. Hyperphosphorylation causes bound tau to dissociate from microtubules as free tau. In the process, tau hyperphosphorylation contributes to loss of affinity to their specific microtubule binding domains, which results in their collapse, which in turn, disrupts the neuronal cytoskeleton and renders the neuronal transportation system inefficient [33]. Free tau within the neuronal soma converts to PHFs and/or SF with variable filament sizes [34]. Kanagasingam et al. [35] mapped VQIVYK, VQIINK motifs in the gingipains'-fragmented tau peptides [10] to their microtubule binding domains in PHFs and SFs [35]. This is an important domain linking PHFs and SFs to the NFT lesion.

Host enzymes implicated in phosphorylating tau include CDK5, casein kinase 1δ, casein kinase 2, cyclic AMP dependent protein kinase, and GSK-3β [30, 31]. The mechanism of hyperphosphorylation of tau via *P. gingivalis* suggests either its infection and/or virulence factors (LPS, gingipains) induce signaling pathways that can indirectly activate GSK-3β *in vitro* and *in vivo* [36–38], which in turn, could be phosphorylating *de novo* tau at ser396 and thr231 residues as already reported [23, 24].

The aims of the present study were to determine the action of gingipains'-fragmented tau peptides for their antimicrobial properties on *P. gingivalis* planktonic cultures and to assess the secondary and tertiary structures of tau containing "VQIINK" and "VQIVYK" hexapeptide motifs, for PHFs and/or SF. The overall rationale was to forge causal links of gingipains'-fragmented tau peptides with PHFs and SFs to the NFT lesion and AD, and in turn, gingipains to tau and periodontal disease.

MATERIALS AND METHODS

Porphyromonas gingivalis cultures

P. gingivalis ATCC 33277™ was cultured for 26 h in Tryptone soya broth (TSB) supplemented with hemin (5 mg/L) and menadione (1 mg/L) (Sigma-Aldrich, UK) in an anaerobic workstation (Don Whitely Scientific, UK) set at 37°C temperature and under an atmosphere of 5% H_2, 5% Co_2, and 90% N_2 to achieve log phase growth to an optical density (OD) of 0.240 at 660 nm. Planktonic cells were diluted down to 10^{-6} in sterile Ringer's buffer (Sigma-Aldrich, UK) to obtain colony-forming units per milliliter (cfu/mL) using the countable range of 30–300 colonies. Subsequently, a surface drop method [39] was employed, using fixed volume aliquots (20 µl) of *P. gingivalis*, of a 1×10^{-4} diluted cell suspension (in triplicate), onto the surface of freshly poured, dried and pre-labelled Tryptone soya agar supplemented with hemin (5 mg/L), menadione (1 mg/L) (Sigma-Aldrich, UK) and 10% defibrinated, oxalated horse blood (Oxoid SR0050) referred to as blood agar plates (BAP).

Assessment of the putative gingipain binding tau hexapeptide motif antimicrobial activity on P. gingivalis

Stock concentrations (1 mM) of peptides designated A-G (non-phosphorylated) and A-C (phosphorylated) (Table 1) were freshly prepared in ¼ strength sterile Ringers (Sigma-Aldrich, UK) on each day of the experiments. *P. gingivalis* in cell suspension diluted down to 1×10^{-4} was prepared in sufficient volume for test peptides and controls. Working dilutions of each peptide assessed in triplicate were at concentrations of 750 µM (where possible), 500 µM, 333 µM, 150 µM, 50 µM, and 10 µM were made in *P. gingivalis* cell suspension (diluted down to 1×10^{-4}). An equal volume (20 µl) was placed on to their respective BAP media (freshly prepared in-house). Controls consisted of a fixed volume (20 µl) of the same *P. gingivalis* cell suspension diluted down to 1×10^{-4} without peptides to which an equivalent volume of sterile ¼ strength sterile Ringers was added to compensate for the difference in volume of stock peptide initially used to dilute peptide at the required concentration) onto BAP medium as for the test peptide plates. Following incubation for 72 h under anaerobic conditions at 37°C, the plates were checked for discrete colonies within the range of 30–300. Cfu/mL were calculated according to the appropriate dilution factor using the formula:

$$\text{cfu/mL} = \frac{\text{Average number of colonies} \times 10 \times 5}{\text{dilution factor } (1 \times 10^4)}$$

(1)

Table 1

Tau peptides N = 7 (A-G) of interest in this study taken from Dominy et al. [10] and the putative phosphorylated residues (green) as reported by Kanagasingam et al. [35]. VQIINK and VQIVYK motifs indicate paired helical filament containing regions of tau constituting neurofibrillary tangles that bind to microtubule binding domains. They were commercially synthesized and supplied by Severn Biotech Limited, (UK) in their purified crystallized (powder) form with/without posttranslational modification

Designated letter	Region in Tau N-C termini	Peptide sequence identity in full length tau (for those investigated in this study)
A	R211-R221	Non-phosphorylated-TPSLPTPPTR
		Phosphorylated-211TPSLPTPPTR220
B	K259-K290	Non-phosphorylated-HQPGGGK**VQIINK**KLDLSNVQSK
		Phosphorylated-267HQPGGGK**VQIINK**KLDLSNVQSS^{184}K287
C	K28-K290	Non-phosphorylated-**VQIINK**KLDLSNVQSK
		Phosphorylated-275**VQIINK**KLDLSNVQSS^{184}K285
D	K298-K317	Non-phosphorylated-HVPGGGS**VQIVYK**PVDLSK
E	K298-K321	Non-phosphorylated-HVPGGGS**VQIVYK**PVDLSKVTSK
F	K294-K321	Non-phosphorylated-DNIKHVPGGGS**VQIVYK**PVDLSKVTSK
G	R406-K438	Non-phosphorylated-HLSNVSSTGSIDMVDSPQLATLADEVSALAK

Birefringence of tau peptides following Congo Red uptake

Light microscopy

Droplets (25 μL) of non-phosphorylated and phosphorylated-tau reconstituted peptides were placed onto Vectabond™-treated glass slides and allowed to air dry. Peptides were stained with Congo Red and mounted in Gurr's neutral mounting medium under a coverslip and examined for the presence of green birefringence through crossed polarizers on an Olympus BX51 light microscope (Olympus Optical Co. UK, Ltd) at a wavelength range of 455 to 600 nm. Photomicrographs were captured with a Zeiss Axiocam and Axiovision software (Carl Zeiss Vision GmbH, Hallbergmoos, Germany).

Circular dichroism for the structure of the soluble tau peptide A in non-phosphorylated and phosphorylated states

Circular dichroism spectra of tau peptides A in both its non-phosphorylated and phosphorylated forms were diluted (0.01 mg/mL) in either neutral pH PBS or 50% 2,2,2-TFE and their absorbance was measured using a Jasco J-815 fluorescent spectrophotometer (JASCO Deutschland GmbH, Germany) with a 1-mm path-length in a quartz cuvette to minimize any non-specific absorbance. Ten scans were averaged for each sample over a wavelength range of 180–260 nm at 0.5 nm intervals. A bandwidth of 1 nm, and a scan speed of 100 nm/min was used. The averaged blank spectra from PBS alone were subtracted from the test peptides. For secondary structure estimation, CD spectra were deconvoluted using the SELCON 3 Algorithm (protein reference set 3) [40, 41] on the DichroWeb [42–44].

Transmission electron microscopy (TEM)

Droplets (50 μL) of reconstituted peptides in the $^1/_4$ strength sterile Ringer's buffer were dispensed onto Nescofilm (Bando Chemical Industries Ltd. Kobe, Japan) in a humidified incubation chamber. Formvar/carbon coated nickel grids (400 mesh) were floated, film side down, on droplets of each supernatant for 20 min, transferred to 1% glutaraldehyde in neutral pH, 0.01 M phosphate buffered saline (PBS) for 10 min, and washed by placing on droplets of PBS (3 × 1 minute) and further washed in reverse osmosis-purified water for 6 × 1 min. Grids were then transferred to 2% uranium acetate for 10 min [45], lifted off with fine forceps, excess stain solution drained with Whatman 50 filter paper, and grids were allowed to air dry. Samples were examined in a Hitachi HT7800 TEM (Hitachi High Tech Ltd., UK) at 100 kV and images were captured with Radius software (EMSIS GmbH, Germany).

Statistical analysis

Where possible, the data was analyzed using the Statistical Package for the Social Sciences (SPSS). The data was non-parametric, and the Mann Whitney U test was used to determine the differences between two independent groups by comparing the mean cfu/mL of each of the peptides with the corresponding controls at all dilutions for antimicrobial activity. A statistical probability (p value), less than or equal to ≤ 0.05 was considered significant.
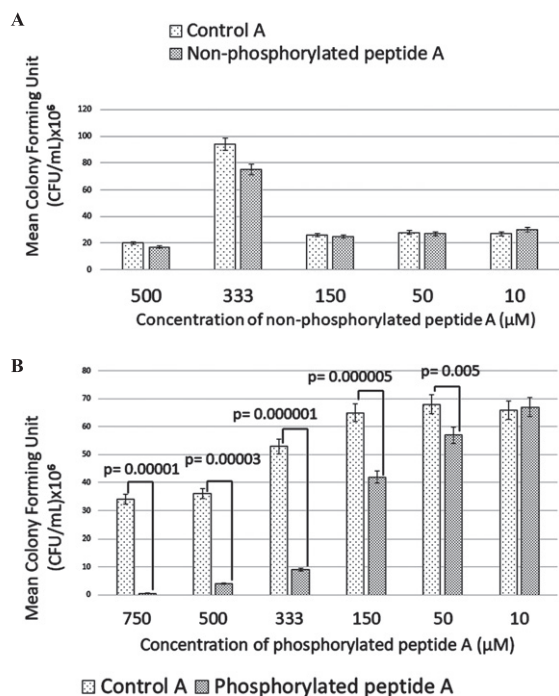
A

B

Fig. 1. Antimicrobial activity of peptide A in non-phosphorylation and phosphorylation state on *P. gingivalis*. A) Non-phosphorylated peptide A. Bar chart to show the growth of viable *P. gingivalis* (cfu/mL) at varying concentrations of peptide A versus bacterial growth without peptide (panel A). There was no statistical difference (*p* value greater than 0.05) in each of the non-phosphorylated peptides A-G compared to the control (without drug), as determined by the non-parametric Mann Whitney U test. Error bars represent standard error of mean. B) Phosphorylated peptide A. Bar chart as in panel A. Phosphorylated peptide A (panel B) demonstrated highly significant statistical difference (*p* = 0.0000) in the phosphorylated peptide A compared to the control (without drug) as determined by the non-parametric Mann Whitney U test across the range of dilutions tested. Error bars as for panel A.

RESULTS

Assessment of the putative gingipain binding hexapeptide motif antimicrobial activity on P. gingivalis

Antimicrobial activity of non-phosphorylated peptides A-G against *P. gingivalis* demonstrated no statistical difference compared to the control (*P. gingivalis* without peptide). An example result is shown for peptide A (Fig. 1A).

A highly significant statistical difference (*p* = 0.0000, Fig. 1B) was seen in the phosphorylated peptide A compared to the control (*P. gingivalis* without peptide) as determined by the non-parametric Mann Whitney U test. Therefore,

phosphorylated peptide A is acting as an antimicrobial agent on *P. gingivalis* across a range of micromolar concentrations (Fig. 1B). No statistical difference was observed for antimicrobial activity of the phosphorylated peptides B and C on *P. gingivalis* planktonic cultures.

Birefringence of tau peptides under crossed polarizers

Peptides A phosphorylated and non-phosphorylated, and peptide G non-phosphorylated forms were not retained on the glass slide because they were soluble and kept washing off making further investigations impossible. All peptides B-F in non-phosphorylated forms and peptides B-C phosphorylated forms displayed apple green birefringence when viewed through crossed polarizers over a wavelength range of 455 to 600 nm. In the non-phosphorylated form, peptide B appeared to have a random fibrillar appearance with blue/green hue or birefringence (Fig. 2A). The phosphorylated peptide B formed a lattice-like crystal structure, remained birefringent with a deeper green shade (Fig. 2B), compared with its non-phosphorylated form shown in Fig. 2A. In its non-phosphorylated state, peptide C appeared to have a lattice crystal structure, that gave apple green hue (Fig. 2C). In its phosphorylated state, peptide C (Fig. 2D) exhibited blue/green birefringence with random aggregating short fibrils. Tau peptide D in its non-phosphorylated state (Fig. 2E) gave greenish birefringence with some lattice structure. Non-phosphorylated tau peptides E and F (Fig. 2F, G) gave greenish birefringence in aggregated clumps without any lattice structures.

Assessment of the secondary structure of the soluble peptide A in non-phosphorylated and phosphorylated forms using circular dichroism

The secondary structure of the soluble tau peptide A in its phosphorylated form using CD spectroscopy (Fig. 3) demonstrated that in aqueous solution, peptide A adopted, a conformation consisting of mainly β-type structures with low levels of α-helix in solution (<15%). In the presence of TFE, the CD spectra confirmed that both forms of peptide A structures were typical of a mixture of α-helical (<15%) and random coil structures with a maxima peak at 198 nm and a negative broad band at 207 nm that indicated partial antiparallel β-sheet structures. Further anal-
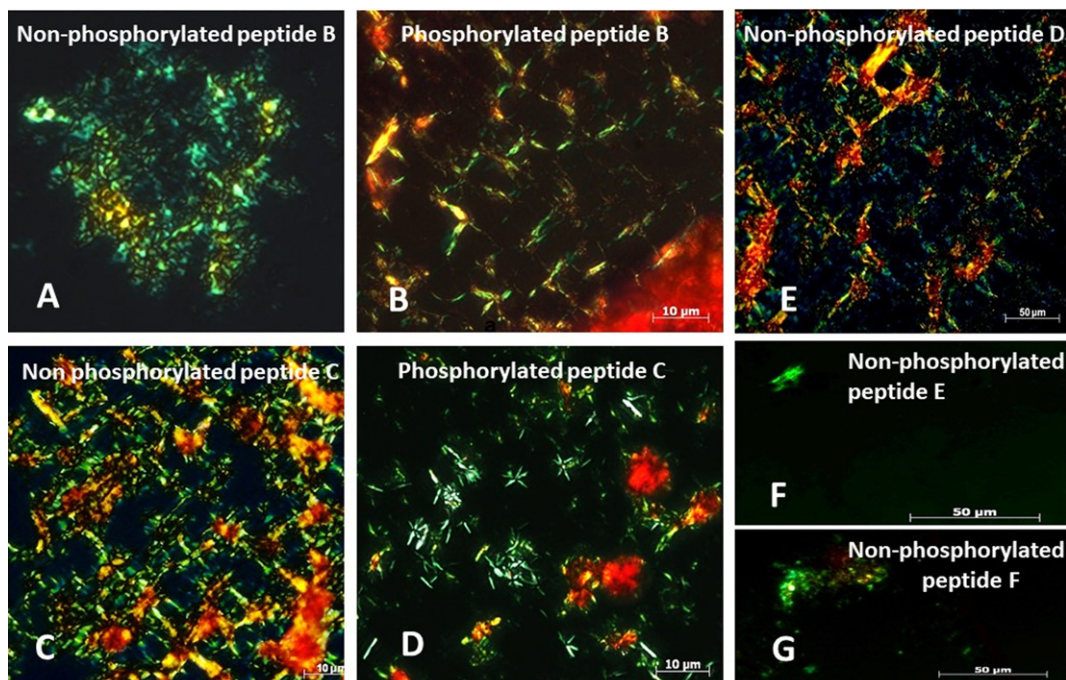
Fig. 2. Polarizing light microscopy following Congo Red staining shows its apple green birefringence in peptides B and C in their non-phosphorylated and phosphorylated states and peptides D-F in their non-phosphorylated form. Tau peptide B in its non-phosphorylated state (panel A) aggregated to give blue/green birefringence. In the phosphorylated form, peptide B remained birefringent with deeper green shade (panel B). The peptide C in its non-phosphorylated state appeared with lattice crystal structure and gave apple green birefringence (panel C). In its phosphorylated state, peptide C (panel D) gave blue/greenish birefringence and the lattice structure appeared to have been disrupted. Tau peptide D in its non-phosphorylated state (panel E) gave greenish birefringence with some lattice structure. Non-phosphorylated tau peptides E and F (panels F and G) gave greenish birefringence in aggregated clumps without any lattice structures.

ysis of the spectra using SELCON 3 showed that this structure was mainly of unordered, β-sheet type (Table 3). The presence of TFE which was used to stabilize the secondary structure, demonstrated a strong negative band at 198 nm and 203 nm, which is characteristic of a "turn" within the peptide representing an anti-parallel β-sheet structure.

Secondary and tertiary structure of peptides B-F by TEM

Tau peptides A and G

For tau peptide A, both non-phosphorylated and phosphorylated forms and peptide G non-phosphorylated form it was found that, there was no adsorption of the protein to the support film and further analysis by TEM was abandoned.

Non-phosphorylated tau peptide B demonstrated long (mean length 1164 nm range 500–2000 nm) fibrils forming random aggregates, some fibers displayed a clear and consistent distance along the twisted repeat morphology (dimensions not calcu-

lated) (Fig. 4A, black arrows). The phosphorylation of peptide B also showed long fibrils, but their helical repeats decreased significantly along the fiber length (Fig. 4B) compared with the non-phosphorylated form shown in Fig. 4A.

Non-phosphorylated tau peptide C ultrastructure mostly demonstrated short (mean length 439 nm range 143–725 nm) fibrils (Fig. 4C), although there was the odd longer fibril that appeared to be randomly aggregating with shorter fibrils in the process of forming twists (Fig. 4C arrows). The phosphorylated peptide C predominantly demonstrated thickened fibrils (Fig. 4D) compared with the non-phosphorylated peptide C shown in Fig. 4C. The phosphorylated peptide C fibrils showed helical twists (anti-parallel β-sheet structure) along all of its fiber length(s) (Fig. 4D, black arrows) that were of a clear and consistent distance from each twist. Although, not measured, the twists in the phosphorylated tau peptide C were much tighter as compared to the periodicity of the twists observed in the non-phosphorylated tau peptide B.
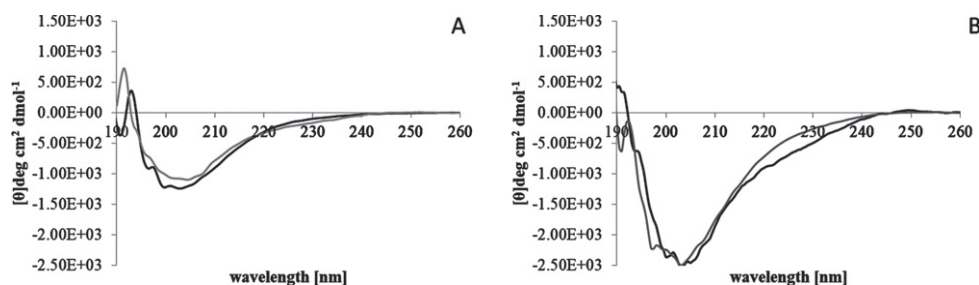
Fig. 3. Circular dichroism spectroscopic analysis of tau peptide A. Non-phosphorylated peptide A (panel A) and phosphorylated peptide A (panel B) show circular dichroism spectra in the presence of PBS (black) and TFE (grey).

The non-phosphorylated tau peptide D demonstrated short (mean length 391 nm range 136–655 nm) straight fibrils (Fig. 4E). Tau peptide E was of medium length (mean length 658 nm range 200–1500 nm) fibrils, with random aggregates (Fig. 4F). Tau peptide F formed long fibrils (mean length 1100 nm range 200–5097 nm) with very few aggregates displaying helical twists within the fibrils (Fig. 4G). Overall, all the fibrils from peptides B-F bearing VQIINK and VQIVYK hexapeptide motifs demonstrated twists whereby some twists were more obvious than others.

DISCUSSION

P. gingivalis is a keystone periodontal disease pathogen [27] and produces gingipains, which are classified as collagenases and trypsin-like cysteine proteinases capable of cleaving tau protein into several peptides [10]. This has implications for AD neuropathology because the activity of intra neuronal gingipains could be a source of free tau. The implication here is that free tau will give rise to PHF and SF, if cleaved from the microtubule binding domains because they undergo self-aggregation and become incorporated into NFTs [30, 34]. NFTs are hyper-phosphorylated tau and one of the two diagnostic lesions of AD. NFTs are linked to Braak staging and progression of AD [17]. They spread in a predictable pattern to involve connecting neurons that project between the individual cortical regions and hippocampus, amygdala, and association cortices of the frontal, temporal, and parietal lobes and possibly in reverse order from the locus coeruleus [17, 46].

In the present study, gingipains'-fragmented tau peptides containing "VQIINK" and "VQIVYK" hexapeptide motifs, which form helical twists *in vivo*, retained their propensity to form tertiary structures *ex vivo*. The tertiary structure seen in peptides B-C,

therefore equate to PHFs and SF *in vitro*. The difference in roles between soluble peptides A and G would be better explained in terms of their behavior under physiological conditions where they may be involved in promoting the formation, elongation, maintenance, and stability of structural microtubules [47]. The insoluble peptides B-E with their ability to form PHF and SF appear to have a role in forming cytoskeletal pathology leading to NFT formation in AD [47]. To elucidate the interactions between the tau peptides and *P. gingivalis*, several, antimicrobial assays were undertaken to explain the mechanism of killing this oral bacterium. The first step in the antimicrobial action of tau peptide A against the *P. gingivalis* bacterium is its outer membrane permeabilization. The minimum lethal concentration of phosphorylated peptide A was within a range of 750 to 50 μM [14]. However, Kobayashi et al. [14] tested their peptides on *Staphylococcus aureus* (Gram-positive), *Escherichia coli* (Gram-negative), and *Candida albicans* using very different antibacterial assays. The present study tested antimicrobial activity against *P. gingivalis*. Although *P. gingivalis* is also a Gram-negative bacterium, it has differences in its outer membrane composition, making it impossible to compare the concentrations obtained in the two different studies [14].

It can also be argued that *P. gingivalis* ATCC 33277 strain can shield the antigenic structures that are crucial in the interaction between the bacterium and antimicrobials [48]. It appears that *P. gingivalis* is not easily eradicated due to the keystone status of this bacterium as a microbial "persister" [27, 49, 50]. The persister phenomenon of *P. gingivalis* is an adaptive mechanism that increases its survival under lethal doses of antimicrobial compounds by becoming dormant even in the planktonic phase. As a result, the persister form of the bacterium can revive when the effect of the antimicrobial
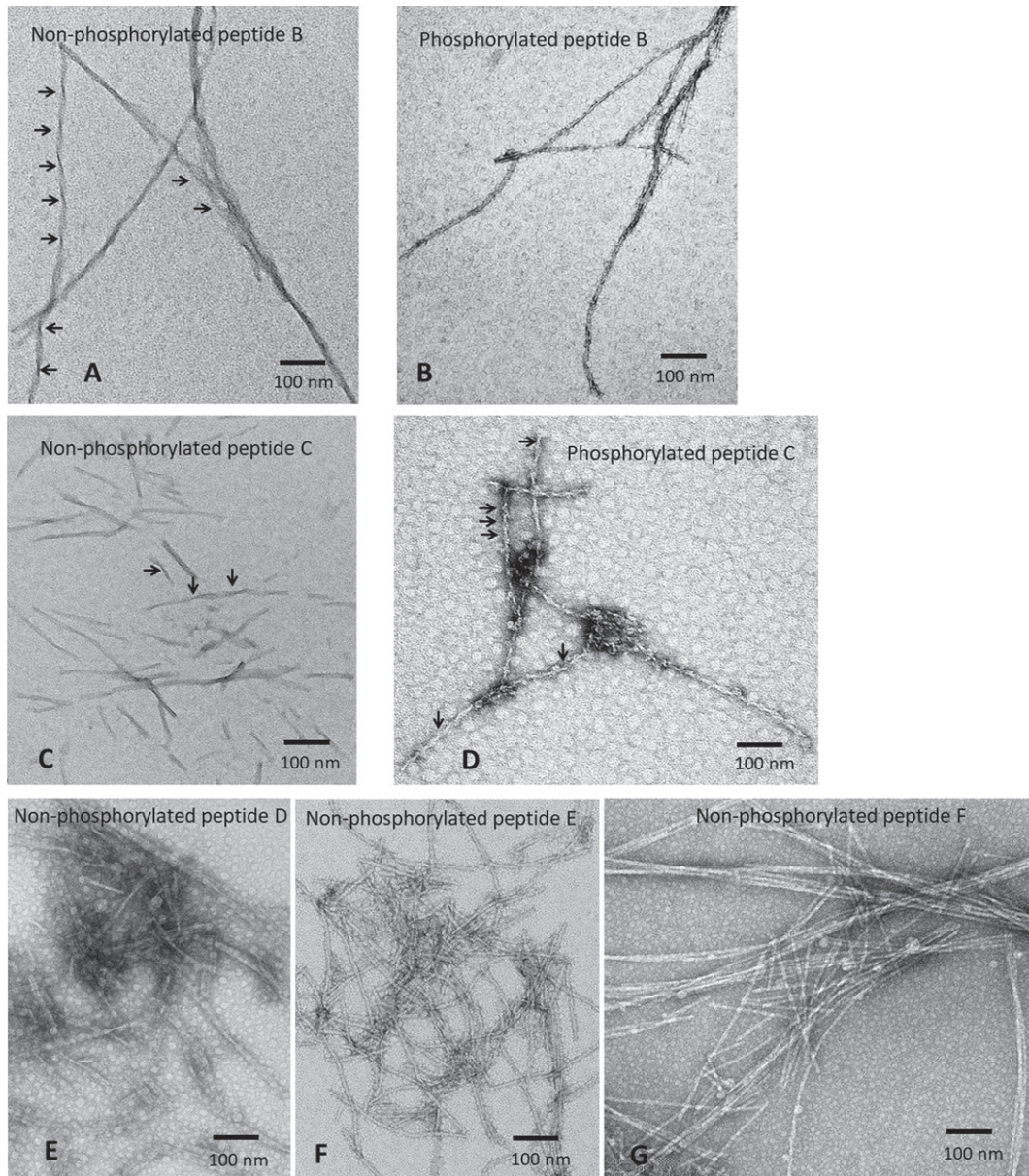
Fig. 4. Tau peptide B in its non-phosphorylated state showed long fibrils with clear and consistent periodicity of twists (panel A, black arrows). In the phosphorylated state, peptide B remained fibrillar, but its helical turns were less defined although they are present (panel B). Micron bar = 100 nm. Tau peptide C in its non-phosphorylated state appeared as shorter fibrils, not fully assembled into fibers and with fewer twists (panel C, arrows). In the phosphorylated state, peptide C remained fibrillar and demonstrated numerous clear, consistent twists throughout all the fibers along their length that appeared to be tighter than those seen at the same magnification for tau peptide B in its non-phosphorylated state shown in panel A black arrows, to become like paired helical structure (4D, black arrows). Micron bar = 100 nm. Non-phosphorylated tau peptides D, E, and F (panels E-G). Peptide D in its non-phosphorylated state appeared as short and long fibrils randomly arranged without twists and some clustering suggesting it may be hydrophobic (panel E). Peptide E in its non-phosphorylated state appeared as random clusters suggestive of hydrophobic interaction with other fibrils composed of short and some long fibrils without clear twists (panel F). Peptide E in its non-phosphorylated state appeared with longer strands of fibrils suggestive of short fibrils joining up to form longer fibers (panel G). Micron bar = 100 nm.

treatment expires. This potential mechanism of protection may be due to its membrane phospholipid composition which is enhanced in phosphatidylglyc-

erol over phosphatidylethanolamine [51]. However, we did find enhanced killing of planktonic *P. gingivalis* with only few persister cell colonies surviving

at lethal doses (750 μM to 50 μM) of phosphorylated peptide A, which has three amino acid residues out of ten which are prone to phosphorylation and is soluble. Since, phosphorylation lowers the pH of the peptide solution, this may have contributed to the killing of *P. gingivalis*, which has been reported to grow within the narrow optimal pH range of 6.5–7.0 [52]. Interestingly, researchers have shown that AD is associated with a decreased pH of the brain and cerebrospinal fluid [53]. If this is the case, then the laboratory conditions in this study may not have been dissimilar to the *in vivo* state of the AD brain. Therefore, a possible link may exist between tau as a substrate for gingipains remains with PHF and SF in NFT formation [10].

In vivo experimental models have suggested that LPS from oral, Gram-negative bacteria especially *P. gingivalis* does have a role in chronic local inflammation [54], increasing cognitive decline [55] and tau protein cleavage from its bound state to microtubules and phosphorylation [10, 23, 24, 35, 56]. Phosphorylation of tau protein by GSK-β activation is supported by our own gene array data from *in vitro* application of *P. gingivalis* LPS to the neuroblastoma IMR-32 cells [37] and *in vivo* animal model of periodontitis for investigating AD [38].

In the present study, we tested one peptide from the proline-rich domain (peptide A), which in an AD brain contains many residues prone to phosphorylation. Peptides B-F were from the microtubule binding domains with VQIINK and VQIVYK motifs which harbor PHFs and residues prone to phosphorylation and peptide G from the C-terminal domain with at least 8 serine and threonine sites prone to phosphorylation. All peptides contain residues such as threonine and serine which are prone to phosphorylation. It is known that excessive phosphorylation causes the normally soluble tau to become insoluble [53] and subsequently affects the physicochemical properties of the peptides leading to conformational changes. Due to spontaneous and uncontrolled aggregation of free and/or phosphorylated tau, NFTs are considered toxic to nerve cells.

Kobayashi et al. [14] did not report their secondary or tertiary structures for any of the short peptides. Their focus was on testing the antimicrobial properties against *S. aureus*, *E. coli*, and *C. albicans* using very different antibacterial assays. It was apparent that the peptide motifs studied by Kobayashi et al. [14] not only consisted largely of polar amino acids, but also had an unprotected α-amino group and the carboxylic acid terminus, which are prone to retaining

positive and negative charges respectively. In larger peptides/proteins those functional groups would normally contribute to the intermolecular hydrogen bonding, and consequently self-assembly. In the case of shorter peptides, as those reported by Kobayashi et al. [14], the functional groups would have remained uninterrupted with a potential for interference with bacterial viability.

During this study peptides B and C (phosphorylated and non-phosphorylated) D, E F (non-phosphorylated) were found to self-assemble and to form fibrillar structures (TEM). Even though peptides B-F consist of either VQIVYK or VQIINK antimicrobial motif, they did not show any antimicrobial activity against *P. gingivalis*. It is our understanding, that the functional groups that are contributing to the antimicrobial properties of the peptide become inactive during the intermolecular hydrogen bonding and self-assembly into fibrillar structure.

Alternatively, Divry [57] showed that the center of many Aβ plaques, based upon their histochemical reactions with Congo Red stain, are birefringent under polarized light. In the present study, we attempted to evaluate the birefringence properties to tau. The present *ex vivo* study used pure tau and the results clearly demonstrated birefringence at the same polarizing light wavelength characteristic for insoluble Aβ.

In vivo studies however, which are based on the understanding of amyloid precursor gene (APP) processing, infers that APP is processed via either of the non-amyloidogenic or the amyloidogenic pathways, both of which generate soluble ectodomains (sAPPα and sAPPβ) and identical intracellular C-terminal fragments (AICD). Of these, the AICD domain is detected by anti-amyloid antibodies [6, 58]. Therefore, the possibility of intraneuronal amyloid being present in the NFT-bearing neurons means that either amyloid or tau, or both, are showing birefringence.

Pure tau also presented an opportunity to test whether the helical twists occur *ex vivo* as Terry [15] considered, the NFT to be composed of twisted tubules or as Kidd [59] suggested, that they were paired filaments arranged in a double helix with intermittent narrowing of a specific periodicity. Our results appear to agree with Terry [15] and Kidd [59] in that they form helical repeats or twists (dimensions not measured), but they appeared fibrillar rather than tubular *ex vivo* under the TEM. The present study also shows that physicochemical properties of non/phosphorylated tau can decrease and/or increase the "twists" along a fibril. As the dimensions of the

Table 2
An initial non-phosphorylated peptide toxicity prediction carried out by Severn Biotech Ltd., UK

Region in Tau N-C termini	Peptides A-G	Toxic?	No of residues	Charge
R211-R221	TPSLPTPPTR	No	10	+1
K259-K290	HQPGGGK**VQIINK**KLDLSNVQSK	Yes	23	+3
K28-K290	**VQIINK**KLDLSNVQSK	Yes	16	+2
K298-K317	HVPGGGS**VQIVYK**PVDLSK	Yes	19	+1.09
K298-K321	HVPGGGS**VQIVYK**PVDLSKVTSK	Yes	23	+2
K294-K317	DNIKHVPGGGS**VQIVYK**PVDLSK	Yes	23	+1.09
K294-K321	DNIKHVPGGGS**VQIVYK**PVDLSKVTSK	Yes	27	+2

Table 3
Secondary structure determination of tau peptide A in its non- phosphorylated and phosphorylated states

Peptide A	Conditions	Helix	Strand	Turns	Unordered
Non-phosphorylated	1 × PBS	15.2	32.2	22.2	34.9
Non-phosphorylated	50% TFE	13.7	32.4	21.5	34.5
Phosphorylated	1 × PBS	13.4	31.7	21.2	34.1
Phosphorylated	50% TFE	13.5	32.7	21.5	34.3

twists were not measured, the authors of this study are unable to determine whether they represent the same ultrastructural properties of their periodicity or by twist width, as those previously reported by Terry [15]. Nevertheless, twists were present in both non-phosphorylated or the phosphorylated state, which seemed to be of a slightly different (loose or tight) configuration, depending on their post-translational status, as observed in this study.

Investigations of mammalian cells *in vitro* and *in vivo* animal models following *P. gingivalis* infection suggests many of the kinases and phosphatases including GSK-3β involved in tau phosphorylation are activated via signal transduction pathways and phosphorylation of tau by GSK-3β following *P. gingivalis* infection [23, 24, 37, 38]. Therefore, *P. gingivalis*, a keystone pathogen of periodontal disease is a strong risk factor for AD as suggested previously by Kanagasingam et al. [35].

The peptides chosen for testing were decided upon in the first case by their ability to represent the tau containing "VQIINK" and "VQIVYK" hexapeptide [10]. This is because they were mapped according to their microtubule binding domains in PHFs and SFs linking back to the NFT lesion [35]. This lesion is related to the Braak staging and disease severity. Hence, these peptides are relevant to the neuropathology of AD. An initial peptide toxicity prediction was then requested from the Severn Biotech Limited, UK (Table 3), the company that initially synthesized the non-phosphorylated peptides, before undertaking further laboratory testing. The antimicrobial predic-

tion program suggested that peptide A would not be toxic and therefore was chosen as a control peptide for those that were predicted to be toxic, bearing the VQIINK and VQIVYK motifs (Table 2). Our results suggest that phosphorylated peptide A did reduce *P. gingivalis* numbers at the 750 to 50 μM range of concentrations and our explanation for this differing expectation is that a prediction tool used to generate the antimicrobial properties in this instance can only be regarded as being theoretical.

Future research

Further research on antimicrobial peptides

Dominy et al. [10] reported nine possible tau peptides cleaved by gingipains. Here we investigated seven tau peptides. Further research needs to be undertaken to investigate the structure of the remaining two peptides, which were not investigated here. Once the structures of the peptides are confirmed, the research could be expanded to investigate the binding of all nine tau peptides to bacterial membranes as described by Jung et al. [60]. Wall et al. [61] devised a model using liposomes for investigating the ability of a peptide binding to a model membrane when the peptide lacks a tryptophan residue using a fluorescein-phosphatidylethanolamine (FPE) probe [60–63]. Based on these studies the antimicrobial action of the peptides will give an insight into their ability to bind to the membranes of target organisms which may involve specific lipids or membrane receptors.

Assessment of the cytotoxicity of the hexapeptide and other motifs

This should be carried out on differentiated neuronal cells *in vitro* for up to 72 h time points with exposure to the various concentrations of tau peptides in triplicate with a known toxic compound as a control.

Conclusions

The tertiary structure of tau peptides B-C (non-phosphorylated and phosphorylated forms) confirms physical changes caused by post-translational modification. TEM of peptides B-F gives some information about the PHF/SF ability to self-aggregate and become incorporated to form longer fibers. The phosphorylated tau peptide C with clear stacking and twisting of the fibers suggests significant hydrophobicity on the external part of the fiber. This may contribute to further aggregation of PHF or SF to form larger aggregates and bundles of filaments leading to NFT formation. Peptides B-F in their non-phosphorylated and peptides B-C in their phosphorylated states displayed mainly β-sheet type structures and this correlates with their birefringence. A shared characteristic of tau with Aβ. A possible link with tau, as a substrate for gingipains, is strengthened via *ex vivo* formation of PHF and SF linking back to NFTs.

The pathological relevance of the present study is the plausibility of free tau being released, by gingipains, from microtubules. Eventual death of the neuron would release the free tau into the cerebral parenchyma and activate the innate immune responses and contribute to neuroinflammation [64–66]. Free tau could also be spreading to connecting neurons [67].

Overall, there is a basis for prevention by removal of the potential causative agent if that is *P. gingivalis* or its gingipains at the primary (oral) site.

REFERENCES

[1] Foguem C, Manckoundia P (2018) Lewy body disease: Clinical and pathological "overlap syndrome" between synucleinopathies (Parkinson disease) and tauopathies (Alzheimer's disease). *Curr Neurol Neurosci Rep* **18**, 24

[2] Salehi A, Ashford JW, Mufson EJ (2016) The link between Alzheimer's disease and Down syndrome. A historical perspective. *Curr Alzheimer Res* **13**, 2-6.

[3] Luchsinger JA, Tang MX, Stern Y, Shea S, Mayeux R (2001) Diabetes mellitus and risk of Alzheimer's disease and dementia with stroke in a multiethnic cohort. *Am J Epidemiol* **154**, 635-641.

[4] de la Torre JC (2006) How do heart disease and stroke become risk factors for Alzheimer's disease? *Neurol Res* **28**, 637-644.

[5] Li L, Cavuoto M, Biddiscombe K, Pike KE (2020) Diabetes mellitus increases risk of incident dementia in APOEε4 carriers: A meta-analysis. *J Alzheimers Dis* **74**, 1295-1308.

[6] Hyman BT, Phelps CH, Beach TG, Bigio EH, Cairns NJ, Carrillo MC, Dickson DW, Duyckaerts C, Frosch MP, Masliah E, Mirra SS, Nelson PT, Schneider JA, Thal DR, Thies B, Trojanowski JQ, Vinters HV, Montine TJ (2012) National institute on aging–Alzheimer's association guidelines for the neuropathologic assessment of Alzheimer's disease. *Alzheimers Dement* **8**, 1-13.

[7] Moir RD, Lathe R, Tanzi RE (2018) The antimicrobial protection hypothesis of Alzheimer's disease. *Alzheimers Dement* **14**, 1602-1614.

[8] Nazir MA (2017) Prevalence of periodontal disease, its association with systemic diseases and prevention. *Int J Health Sci (Qassim)* **11**, 72-80.

[9] Poole S, Singhrao SK, Kesavalu L, Curtis MA, Crean S (2013) Determining the presence of periodontopathic virulence factors in short-term post-mortem Alzheimer's disease brain tissue. *J Alzheimers Dis* **36**, 665-677.

[10] Dominy SS, Lynch C, Ermini F, Benedyk M, Marczyk A, Konradi A, Nguyen M, Haditsch U, Raha D, Griffin C, Holsinger LJ, Arastu-Kapur S, Kaba S, Lee A, Ryder MI, Potempa B, Mydel P, Hellvard A, Adamowicz K, Hasturk H, Walker GD, Reynolds EC, Faull RLM, Curtis MA, Dragunow M, Potempa J (2019) *Porphyromonas gingivalis* in Alzheimer's disease brains: Evidence for disease causation and treatment with small-molecule inhibitors. *Sci Adv* **5**, eaau3333.

[11] Singhrao SK, Olsen I (2018) Are *Porphyromonas gingivalis* outer membrane vesicles, microbullets for sporadic Alzheimer's disease manifestation? *J Alzheimers Dis Rep* **20**, 219-228.

[12] Olsen I, Singhrao SK (2019) Is there a link between genetic defects in the complement cascade and *Porphyromonas gingivalis* in Alzheimer's disease? *J Oral Microbiol* **12**, 167648.

[13] Ryder M, Detke M, Sabbagh M, Bolger J, Hennings D, Skljarevski V, Kapur S, Raha D, Ermini F, Nguyen M, Haditsch U, Perry K, Ritch K, Hendrix S, Dickson S, Hasturk H, Horine S, Mallinckrodt C, Holsinger LJ, Lynch C, Dominy S (2022) A role for *P. gingivalis* in Alzheimer's

disease: Evidence from the GAIN Study (abstract). *4th International Conference on Porphyromonas gingivalis and Related Species in Oral and Systemic Diseases*, Louisville, KY.

[14] Kobayashi N, Masuda J, Kudoh J, Shimizu N, Yoshida T (2008) Binding sites on tau proteins as components for antimicrobial peptides. *Biocontrol Sci* **13**, 49-56.

[15] Terry RD (1963) The fine structure of neurofibrillary tangles in Alzheimer's disease. *J Neuropathol Exp Neurol* **22**, 629-642.

[16] Braak H, Alafuzoff I, Arzberger T, Kretzschmar H, Del Tredici K (2006) Staging of Alzheimer disease-associated neurofibrillary pathology using paraffin sections and immunocytochemistry. *Acta Neuropathol* **112**, 389-404.

[17] Braak H, Thal DR, Ghebremedhin E, Del Tredici K (2011) Stages of the pathologic process in Alzheimer disease: Age categories from 1 to 100 years. *J Neuropathol Exp Neurol* **70**, 960-969.

[18] Sparks Stein P, Steffen MJ, Smith C, Jicha G, Ebersole JL, Abner E, Dawson D 3rd (2012) Serum antibodies to periodontal pathogens are a risk factor for Alzheimer's disease. *Alzheimers Dement* **8**, 196-203.

[19] Chen CK, Wu YT, Chang YC (2017) Association between chronic periodontitis and the risk of Alzheimer's disease: A retrospective, population-based, matched-cohort study. *Alzheimers Res Ther* **9**, 56.

[20] Beydoun MA, Beydoun HA, Hossain S, El-Hajj ZW, Weiss J, Zonderman AB (2020) Clinical and bacterial markers of periodontitis and their association with incident all-cause and Alzheimer's disease dementia in a large national survey. *J Alzheimers Dis* **75**, 157-172.

[21] Zhan X, Stamova B, Sharp FR (2018) Lipopolysaccharide associates with amyloid plaques, neurons and oligodendrocytes in Alzheimer's disease brain: A review. *Front Aging Neurosci* **10**, 42.

[22] Beutler B (2000) Endotoxin, toll-like receptor 4, and the afferent limb of innate immunity. *Curr Opin Microbiol* **3**, 23-28.

[23] Ilievski V, Zuchowska PK, Green SJ, Toth PT, Ragozzino ME, Le K, Aljewari HW, O'Brien-Simpson NM, Reynolds EC, Watanabe K (2018) Chronic oral application of a periodontal pathogen results in brain inflammation, neurodegeneration and amyloid beta production in wild type mice. *PLoS One* **13**, e0204941.

[24] Haditsch U, Roth T, Rodriguez L, Hancock S, Cecere T, Nguyen M, Arastu-Kapur S, Broce S, Raha D, Lynch CC, Holsinger LJ, Dominy SS, Ermini F (2020) Alzheimer's disease-like neurodegeneration in *Porphyromonas gingivalis* infected neurons with persistent expression of active gingipains. *J Alzheimers Dis* **75**, 1361-1376.

[25] Soscia SJ, Kirby JE, Washicosky KJ, Tucker SM, Ingelsson M, Hyman B, Burton MA, Goldstein LE, Duong S, Tanzi RE, Moir RD (2010) The Alzheimer's disease-associated amyloid b-protein is an antimicrobial peptide. *PLoS One* **5**, e9505.

[26] Kumar DK, Choi SH, Washicosky KJ, Eimer WA, Tucker S, Ghofrani J, Lefkowitz A, McColl G, Goldstein LE, Tanzi RE, Moir RD (2016) Amyloid-β peptide protects against microbial infection in mouse and worm models of Alzheimer's disease. *Sci Transl Med* **8**, 340ra72.

[27] Hajishengallis G, Darveau RP, Curtis MA (2012) The keystone-pathogen hypothesis. *Nat Rev Microbiol* **10**, 717-725.

[28] Harris F, Dennison SR, Phoenix DA (2012) Aberrant action of amyloidogenic host defense peptides: A new paradigm to investigate neurodegenerative disorders? *FASEB J* **26**, 1776-1781.

[29] Phoenix DA, Dennison SR, Harris F (2013) Anionic antimicrobial peptides. In *Antimicrobial Peptides*, Phoenix DA, Dennison SR, Harris F, eds. Wiley, Germany, pp. 83-113.

[30] Grundke-Iqbal I, Iqbal K, Tung YC, Quinlan M, Wisniewski HM, Binder LI (1986) Abnormal phosphorylation of the microtubule-associated protein tau (tau) in Alzheimer cytoskeletal pathology. *Proc Natl Acad Sci U S A* **83**, 4913-4917.

[31] Hanger D, Hughes K, Woodgett J, Brion J, Anderton B (1992) Glycogen synthase kinase-3 induces Alzheimer's disease-like phosphorylation of tau: Generation of paired helical filament epitopes and neuronal localisation of the kinase. *Neurosci Lett* **147**, 58-62.

[32] Hanger DP, Byers HL, Wray S, Leung KY, Saxton MJ, Seereeram A, Reynolds CH, Ward MA, Anderton BH (2007) Novel phosphorylation sites in tau from Alzheimer brain support a role for casein kinase 1 in disease pathogenesis. *J Biol Chem* **282**, 23645-23654.

[33] Li B, Chohan M, Grundke-Iqbal I, Iqbal K (2007) Disruption of microtubule network by Alzheimer abnormally hyperphosphorylated tau. *Acta Neuropathol* **113**, 501-511.

[34] Maccioni RB, Cambiazo V (1995) Role of microtubule-associated proteins in the control of microtubule assembly. *Physiol Rev* **75**, 835-864.

[35] Kanagasingam S, Chukkapalli SS, Welbury R, Singhrao SK (2020) *Porphyromonas gingivalis is* a strong risk factor for Alzheimer's disease. *J Alzheimers Dis Rep* **4**, 501-511.

[36] Alvarez A, Munoz JP, Maccioni RB (2001) A cdk5/p35 stable complex is involved in the beta-amyloid induced deregulation of cdk5 activity in hippocampal neurons. *Exp Cell Res* **264**, 266-275.

[37] Bahar B, Singhrao SK (2021) An evaluation of the molecular mode of action of trans-resveratrol in the Porphyromonas gingivalis lipopolysaccharide challenged neuronal cell model. *Mol biol Rep* **48**, 147-156.

[38] Bahar B, Kanagasingam S, Tambuwala MM, Aljabali AAA, Dillon SA, Doaei S, Welbury R, Chukkapalli SS, Singhrao SK (2021) *Porphyromonas gingivalis* (W83) infection induces Alzheimer's disease like pathophysiology in obese and diabetic mice. *J Alzheimers Dis* **82**, 1259-1275.

[39] Miles A, Misra S, Irwin J (1938) The estimation of the bactericidal power of the blood. *Epidemiol Infect* **38**, 732-749.

[40] Sreerama N, Woody RW (1993) A self-consistent method for the analysis of protein secondary structure from circular dicroism. *Anal Biochem* **209**, 32-44.

[41] Sreerama N, Venyaminnov SY, Woody RW (1999) Estimation of the number of alpha-helical and beta-strand segments in proteins using circular dicroism spectroscopy. *Protein Sci* **8**, 370-380.

[42] Whitmore L, Wallace BA (2004) DICHROWEB, an online server for protein secondary structure analyses from circular dichroism spectroscopic data. *Nucleic Acids Res* **32**, W668-W673.

[43] Whitmore L, Wallace BA (2008) protein secondary structure analyses from circular dichroism spectroscopy: Methods and reference databases. *Biopolymers* **89**, 392-400.

[44] Whitmore L, Woollett B, Miles AJ, Janes RW, Wallace BA (2010) The protein circular dichroism data bank, a Web-based site for access to circular dichroism spectroscopic data. *Structure* **18**, 1267-1269.

[45] Bils RF, Hall CE (1962) Electron microscopy of wound-tumor virus. *Virology* **17**, 123-130.

[46] Braak H, Braak E (1991) Neuropathological staging of Alzheimer-related changes. *Acta Neuropathol* **82**, 239-259.

[47] Witman GB, Cleveland DW, Weingarten MD, Kirschner, MW (1976) Tubulin requires tau for growth onto microtubule initiating sites. *Proc Natl Acad Sci U S A* **73**, 4070-4074.

[48] Bachrach G, Altman H, Kolenbrander PE, Chalmers NI, Gabai-Gutner M, Mor A, Friedman M, Steinberg D (2008) Resistance of Porphyromonas gingivalis ATCC 33277 to direct killing by antimicrobial peptides is protease independent. *Antimicrob Agents Chemother* **52**, 638-642.

[49] Li P, Fung YE, Yin X, Seneviratne CJ, Che CM, Jin L (2018) Controlled cellular redox, repressive hemin utilization and adaptive stress responses are crucial to metronidazole tolerance of Porphyromonas gingivalis persisters. *J Clin Periodontol* **45**, 1211-1221.

[50] Wang C, Cheng T, Li X, Jin L (2020) Metronidazole-treated Porphyromonas gingivalis persisters invade human gingival epithelial cells and perturb innate responses. *Antimicrob Agents Chemother* **64**, e02529-19.

[51] Nichols FC, Rojaanasomsith K (2006) *Porphyromonas gingivalis* lipids and diseased dental tissues. *Oral Microbiol Immunol* **21**, 84-92.

[52] Takahashi N, Schachtele CF (1990) Effect of pH on the growth and proteolytic activity of *Porphyromonas gingivalis* and bacteroides intermedius. *J Dent Res* **69**, 1266-1269.

[53] Decker Y, Nemeth E, Schomburg R, Chemla A, Fulop L, Menger MD, Liu Y, Fassbender K (2021) Decreased pH in the aging brain and Alzheimer's disease. *Neurobiol Aging* **101**, 40-49.

[54] DiCarlo G, Wilcock D, Henderson D, Gordon M, Morgan D (2001) Intrahippocampal LPS injections reduce Abeta load in APP+PS1 transgenic mice. *Neurobiol Aging* **22**, 1007-1012.

[55] Wu Z, Ni J, Liu Y, Teeling JL, Takayama F, Collcutt A, Ibbett P, Nakanishi H (2017) Cathepsin B plays a critical role in inducing Alzheimer's disease-like phenotypes following chronic systemic exposure to lipopolysaccharide from *Porphyromonas gingivalis* in mice. *Brain Behav Immun* **65**, 350-361.

[56] Lee DC, Rizer J, Selenica MB, Reid P, Kraft C, Johnson A, Blair L, Gordon MN, Dickey CA, Morgan D (2010) LPS-induced inflammation exacerbates phospho-tau pathology in rTg4510 mice. *J Neuroinflammation* **7**, 56.

[57] Divry P (1927) Etude histochimique des plaques seniles. *J Belg Neurol Psych* **27**, 643-657.

[58] Multhaup G, Huber O, Buee L, Galas MC (2015) Amyloid precursor protein (APP) intracellular fragment (AICD), Aβ42, and tau in nuclear roles. *J Biol Chem* **290**, 23515-23522.

[59] Kidd M (1964) Alzheimer's disease. An electron microscopical study. *Brain* **87**, 307-320.

[60] Jung HH, Yang ST, Sim JY, Lee S, Lee JY, Kim HH, Shin SY, Kim JI (2010) Analysis of the solution structure of the human antibiotic peptide dermcidin and its interaction with phospholipid vesicles. *BMB Rep* **43**, 362-368.

[61] Wall J, Golding CA, Van Veen M, O'Shea P (1995) The use of fluoresceinphosphatidylethanolamine (FPE) as a real-time probe for peptide-membrane interactions. *Mol Membr Biol* **12**, 183-192.

[62] O'Toole PJ, Morrison IE, Cherry RJ (2000) Investigations of spectrin-lipid interactions using fluorescein-phosphatidylethanolamine as a membrane probe. *Biochim Biophys Acta* **1466**, 39-46.

[63] Hawrani A, Howe RA, Walsh TR, Dempsey CE (2010) Thermodynamics of RTA3 peptide binding to membranes and consequences for antimicrobial activity. *Biochim Biophys Acta* **1798**, 1254-1262.

[64] Morales I, Farias G, Maccioni RB (2010) Neuroimmunomodulation in the pathogenesis of Alzheimer's disease. *Neuroimmunomodulation* **17**, 202-204.

[65] Kovac A, Zilka N, Kazmerova Z, Cente M, Zilkova M, Novak M (2011) Misfolded truncated protein tau induces innate immune via MAPK pathway. *J Immunol* **187**, 2732-2739.

[66] Laurent C, Buee L, Blum D (2018) Tau and neuroinflammation: What impact for Alzheimer's disease and tauopathies? *Biomed J* **41**, 21-33.

[67] Dioli C, Patricio P, Trindade R, Pinto LG, Silva JM, Morais M, Ferreiro E, Borges S, Mateus-Pinheiro A, Rodrigues AJ, Sousa N, Bessa JM, Pinto L, Sotiropoulos I (2017) Tau-dependent suppression of adult neurogenesis in the stressed hippocampus. *Mol Psychiatry* **22**, 1110-1118.